

Energetics of point defects in the two-dimensional Wigner crystal

Eric Cockayne and Veit Elser

Laboratory of Atomic and Solid State Physics, Cornell University, Ithaca, New York 14853

(Received 25 June 1990)

The ground-state Coulomb energy and zero-point vibrational energy are calculated numerically for the perfect two-dimensional (2D) Wigner crystal and for a 2D Wigner crystal containing interstitials and vacancies. In the limit of large systems, only the vacancy and the interstitial with threefold rotational symmetry are stable. The scaling of the interaction between like defects with interdefect separation is studied and compared with the predictions of elasticity theory. Each type of point defect lowers the zero-point vibrational energy of the system. The role of point defects in the zero-temperature melting transition is discussed in light of these results.

I. INTRODUCTION

It is well known that a system composed of electrons embedded in a uniform positive background at zero temperature will exhibit a crystalline phase, or Wigner crystal, at low densities and a fluid phase at high densities.¹ Experimentally this system is realized in two dimensions (2D) by electrons above a liquid-helium surface where the existence of the crystalline phase has been well established.² Much theoretical work has sought to determine the electron density at which the phase transition to the fluid phase occurs. Recent Monte Carlo calculations have placed the transition at the density where $r_s \approx 37 \pm 5$.³ Besides the critical density one is also interested in the mechanism of the transition. Is “quantum melting” continuous, like the thermal melting transition, or is it first order? In the event that the transition is continuous, one would like to identify the microscopic mechanism. A natural candidate is the dislocation unbinding process that occurs in the thermal transition. At zero temperature one cannot invoke the entropy from the dislocation positions as a factor which competes with the energy. Instead one must ask whether there is a net lowering of the *zero-point* vibrational energy caused by a dislocation pair that ultimately, at the critical density, overwhelms the energy of the pair. With this perspective, however, there are no obvious criteria that would distinguish dislocations as being particularly adept in lowering the zero-point energy. Thus we are led to consider the simple point defects, vacancies and interstitials, as well. This study was motivated by the work of Fisher, Halperin, and Morf⁴ (FHM) which indicated that the lowest energy point defect was an edge-centered interstitial that promised the possibility of a low zero-point energy because of its nearly continuous translational symmetry⁵ (see Fig. 1). We have repeated the calculation of FHM with more advanced computing resources and find that, in fact, the lowest energy defect is the triangle-centered interstitial—the edge-centered interstitial being classically unstable. We do find that both the stable interstitial and the vacancy lower the average zero-point energy of the system. This lowering, however, is insufficient so that if anharmonic terms (which we do not

calculate) are negligible at $r_s \approx 37$ then our results imply that simple point defect condensation is not a viable mechanism for continuous quantum melting.

II. ELECTRON CRYSTAL ENERGY CALCULATIONS

The electrostatic energy of electrons in a Bravais lattice can be evaluated by means of the Ewald sum for the potential seen by a single electron:

$$\phi(i) = \frac{4\pi}{A_c} \sum_{\mathbf{G} \neq 0} |\mathbf{G}|^{-1} \operatorname{erfc} \left(\frac{|\mathbf{G}|}{\sqrt{2}\eta} \right) - \frac{2}{A_c} \left(\frac{\pi}{\eta} \right)^{1/2} + 2 \sum_{j \neq i} \frac{e}{r_{ij}} \operatorname{erfc}(\sqrt{2}\eta r_{ij}) - 2e \left(\frac{\eta}{\pi} \right)^{1/2}. \quad (1)$$

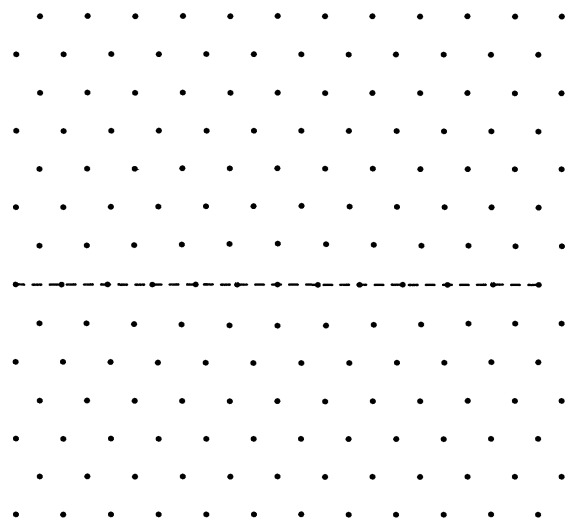


FIG. 1. Wigner crystal containing edge-centered interstitial (EI). Motion of the interstitial along the line indicated is nearly continuous.

Throughout this paper the existence of a uniform neutralizing positive background is assumed. In (1) the sum on \mathbf{G} runs over all reciprocal lattice vectors, j runs over all lattice points, and η is the Ewald parameter which can be adjusted so that both the direct lattice and reciprocal lattice summations converge rapidly. The Coulomb energy per electron is then given by

$$\frac{E_c}{N} = \frac{e}{2} \phi(i), \quad (2)$$

where the factor of $\frac{1}{2}$ compensates for double counting.

For a system composed of a Bravais lattice of unit cells, each with a basis of M electrons, the Ewald sum is modified:

$$\begin{aligned} \phi(i) = & \frac{4\pi}{A_c} \sum_{\mathbf{G} \neq 0} S(\mathbf{G}) |\mathbf{G}|^{-1} \operatorname{erfc} \left[\frac{|\mathbf{G}|}{\sqrt{2\eta}} \right] \\ & - \frac{2}{A_c} \left[\frac{\pi}{\eta} \right]^{1/2} S(\mathbf{0}) \\ & + 2 \sum_{j \neq i} \frac{e}{r_{ij}} \operatorname{erfc}(\sqrt{2\eta} r_{ij}) - 2e \left[\frac{\eta}{\pi} \right]^{1/2}. \end{aligned} \quad (3)$$

The structure factor is given by

$$S(\mathbf{G}) = \sum_{\mathbf{k}} e^{i\mathbf{G} \cdot (\mathbf{r}_{\mathbf{k}} - \mathbf{r}_i)}, \quad (4)$$

where \mathbf{k} runs over all the electrons in the basis. The Coulomb energy per electron is now given by

$$\frac{E_c}{N} = \frac{e}{2} \Phi, \quad \Phi = \frac{1}{M} \sum_{\mathbf{k}} \phi(k), \quad (5)$$

where the sum is again over each electron in the basis.

The zero-point vibrational energy of an N -electron periodic cell in the harmonic approximation is calculated by determining the normal-mode frequencies of the $2N \times 2N$ dynamical matrix

$$C_{i\alpha, j\beta} = \frac{Ne}{2m} \frac{\partial^2 \Phi}{\partial r_{i\alpha} \partial r_{j\beta}} \quad (6)$$

using the differentiated Ewald sum (5). Then the vibrational energy per electron is given by

$$\frac{E_{\text{vib}}}{N} = \frac{\hbar}{2N} \sum_i \omega_i, \quad (7)$$

where $\{\omega_i^2\}$ are the $2N$ eigenvalues of the matrix C . It must be emphasized that this is only an approximation to the zero-point vibrational energy per electron as only the set of normal modes which have the periodicity of the N -electron cell are summed over. An effective method for improving this approximation in the case of the perfect Wigner crystal is given in Sec. III.

As N increases, the evaluation of (3) and (6) becomes increasingly computationally intensive. Minimization of computation time was aided by following a method pointed out by Adams and McDonald^{6,7} of setting the Ewald parameter large enough so that the direct lattice sum had at most one significant contribution from each pair of

electrons in the basis. For the approximately square rectangular unit cells used in this study, 620 terms in the reciprocal lattice were needed for 1 part in 10^{12} accuracy. Furthermore, rather than determine the error function associated with the distance between each pair of electrons, a table of 10 000 such values was created at the beginning of each run, with the value for the pair determined by a parabolic interpolation through the three nearest points of this table. Consistency checks showed that the base potential energy calculations in the present work were good to better than 1 part in 10^{11} .

III. THE PERFECT 2D WIGNER CRYSTAL

The perfect 2D Wigner crystal forms a hexagonal lattice. In the semiclassical approximation, the low-density expansion of the ground-state energy of the crystal may be written in the form

$$\frac{E}{N} = \frac{C_1}{r_s} + \frac{C_{3/2}}{r_s^{3/2}} + O \left[\frac{1}{r_s^2} \right], \quad (8)$$

where E/N is the energy per electron in units of Rydbergs and r_s is the dimensionless radius such that $\pi(r_s a_0)^2$ equals the area per electron A_c , with a_0 the Bohr radius. The first term in the expression represents the equilibrium Coulomb energy, the second term the harmonic term of the zero-point vibrational energy, and the final term the lowest order of the anharmonic oscillator terms.

In all our numerical work we use a rectangular supercell of the hexagonal lattice. In units of the lattice constant a of the hexagonal lattice the length and height of the supercell are m and $n\sqrt{3}$, respectively. In the absence of defects there are $N = 2mn$ electrons in the supercell. Using (3), we find for the hexagonal lattice,

$$\frac{E_c}{N} = -1.960\,515\,8 \frac{e^2}{\sqrt{A_c}}. \quad (9)$$

The final two decimal places differ from the previously published value.⁸ This energy corresponds to $C_1 = -2.212\,205\,2$ above.

The vibrational modes of the perfect 2D crystal are longitudinal and transverse plane waves. We modify the approximate zero-point vibrational energy (7) to label the modes by their longitudinal or transverse nature and their wave vector \mathbf{q} :

$$\frac{E_{\text{vib}}}{N} = \frac{\hbar}{2N} \sum_{\mathbf{q}} [\omega_l(\mathbf{q}) + \omega_t(\mathbf{q})], \quad (10)$$

where the sum runs over all the reciprocal lattice vectors \mathbf{q} of the supercell. Rather than diagonalize the dynamical matrix C to find the normal mode frequencies, we can use the known eigenfunctions $\psi_{\mathbf{q}}^l(r_{j\beta})$ and $\psi_{\mathbf{q}}^t(r_{j\beta})$ for longitudinal and transverse waves to find the frequencies simply via the relations $C\psi_{\mathbf{q}}^{l,t} = (\omega_{\mathbf{q}}^{l,t})^2 \psi_{\mathbf{q}}^{l,t}$. Cunningham has shown⁹ that the most efficient way of evaluating an integral of a function over a Brillouin zone where the function has the full symmetry of the zone is to evaluate the function over a set of special points. The special

points of the hexagonal lattice Brillouin zone correspond to a subset of reciprocal lattice points of a rectangular superlattice having $m = 3^p$ and $n = 3^p$ where p is an integer. Using a set of six special points, Bonsall and Maradudin⁸ found the zero-point vibrational energy per electron in the 2D Wigner crystal to be $4.28 (\hbar\omega_0/2)$ where $\omega_0 = \sqrt{e^2/m\bar{a}^3}$ and \bar{a} is the lattice constant ($A_c = \sqrt{3} \bar{a}^2/2$). Our calculation of the eigenvalues at the larger set of 378 special points yields a coefficient of 4.2776. This corresponds to $C_{3/2} = 1.6274$. In Fig. 2 the phonon dispersion relations are shown as contour plots over the Brillouin zone.

IV. ENERGY OF POINT DEFECTS

Fisher, Halperin, and Morf⁴ identified three simple point defects in the 2D Wigner crystal: the centered interstitial (CI), edge interstitial (EI), and vacancy (V). Any defect must raise the Coulomb energy of the system; if the total ground-state energy of the Wigner crystal with a defect is to be lowered, it must be through a reduction in the zero-point vibrational energy. With the contributions to the energy again solely the Coulomb and zero-point vibrational energies, we expect the energy of a single isolat-

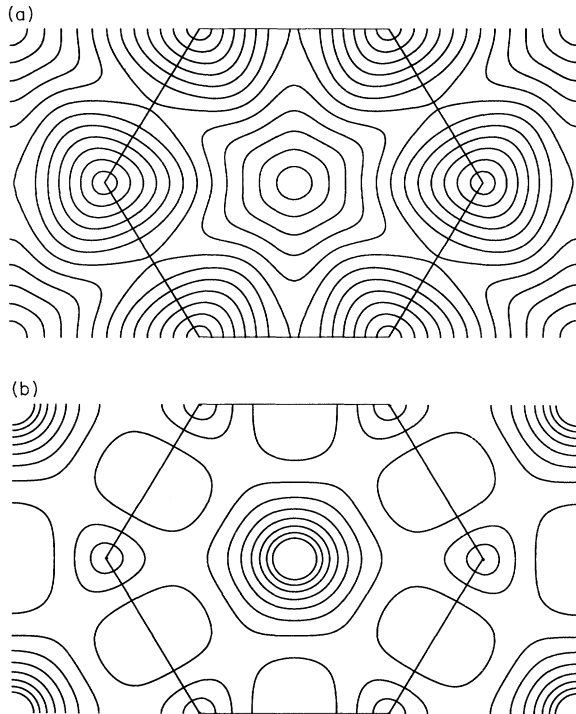


FIG. 2. Phonon dispersion relations $\omega(\mathbf{q})$ for (a) transverse modes and (b) longitudinal modes of the perfect 2D Wigner crystal over the Brillouin zone (BZ). The contour interval is $0.1\omega_0$. For clarity, only contours for $\omega \geq 0.9\omega_0$ are shown for the longitudinal modes. The transverse modes dispersion relation has a minimum at the origin, maxima at the BZ corners, and saddle points at the BZ edge centers. The longitudinal modes dispersion relation has a minimum at the origin, maxima at the BZ edge centers, and local minima at the BZ corners.

ed defect of each type in an otherwise perfect crystal to also be given by an expansion of the form

$$E_{\text{defect}} = \frac{C_1(\text{defect})}{r_s} + \frac{C_{3/2}(\text{defect})}{r_s^{3/2}} + O\left(\frac{1}{r_s^2}\right). \quad (11)$$

We calculate the coefficients $C_1(\text{defect})$ and $C_{3/2}(\text{defect})$ numerically.

A. Coulomb energy

To calculate the Coulomb energy we begin, as before, with a rectangular perfect crystal superlattice, where the parameters $m = 5t$ and $n = 3t$, t integer, are chosen so that the superlattice approximates a square to within 4%. To this system of $2mn = 30t^2$ electrons, an electron is added to create a CI or EI or one is removed to create a vacancy, as shown in Fig. 3. Since it is known that the EI causes relaxation for an extended distance along its own row,^{4,5} the edge interstitial is placed so as to maximize the distance between an EI and its images along its own row. After placing the defect we rescale the dimensions of the supercell by a factor of

$$\left(\frac{2mn \pm 1}{2mn}\right)^{1/2} \quad (12)$$

to reset the system to the initial density. This avoids the complications of having to correct the energy calculations for density changes.⁴

The Coulomb energy per electron of the supercell $(e/2)\Phi$ was determined by explicit evaluation of the Ewald sum (5). After adding the defect, the relaxation and equilibrium energy were computed by writing the energy as a function of the $2N$ particle coordinates and using standard conjugate-gradient methods to minimize this function.¹⁰

After evaluation of the equilibrium Coulomb energy, the Coulomb energy of the defect was determined by subtracting the Coulomb energy of the same number of electrons in a perfect crystal of the same density:

$$E_c(\text{defect}) = \frac{Ne}{2} [\Phi - \Phi(\text{perfect})]. \quad (13)$$

This yielded the Coulomb energy change per defect of a system containing a superlattice of such defects. The iso-

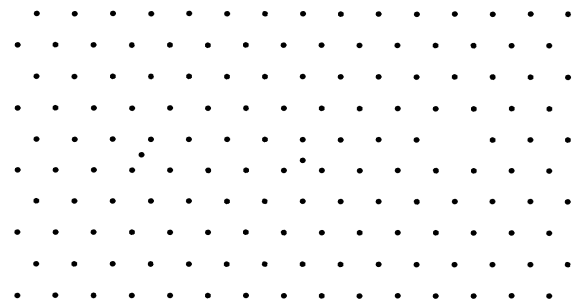


FIG. 3. 2D Wigner crystal containing unrelaxed (left) EI, (center) CI, and (right) V defects.

lated defect energy was computed by calculating the energy for successive t in the supercell size and extrapolating the results to infinite supercell size.

The relaxed configurations for each type of point defect are shown in Fig. 4. The relaxed configurations for the CI and EI maintain the symmetry of the unrelaxed configurations, with the CI configuration just slightly distorted to a lower symmetry by the boundary conditions. The vacancy, however, was found to relax into a configuration of lower symmetry, in contrast to previously reported behavior.⁴

The Coulomb energy per defect in a lattice of unit density is shown as a function of supercell size in Fig. 5, where the horizontal axis for each type of defect is scaled via the elasticity theory prediction of the defect-image interaction, as discussed in Sec. V. Extrapolation to infinite

supercell size yields $E_c(\text{CI})=0.1364$, $E_c(\text{EI})=0.1394$, and $E_c(\text{V})=0.1939$, where the energies are expressed in units of $e^2/\sqrt{A_c}$. Our energy calculations show that, contrary to the results of FHM, the centered interstitial is the lowest energy point defect in the 2D Wigner crystal. These results give $C_1(\text{CI})=0.1539$, $C_1(\text{EI})=0.1573$, and $C_1(\text{V})=0.2188$ in the expansions above. The values given for the EI and V energies are accurate to ± 1 in the last digit given, while the values for the CI energies are accurate to the last digit given.

In addition, it was found that the EI was unstable for even the largest (271 electron) system whose normal modes were computed. The unstable “buckling” mode as shown in Fig. 6 was found to lead to a CI configuration upon relaxation. We conjecture that the EI remains unstable in the limit of an isolated EI, in contrast to the

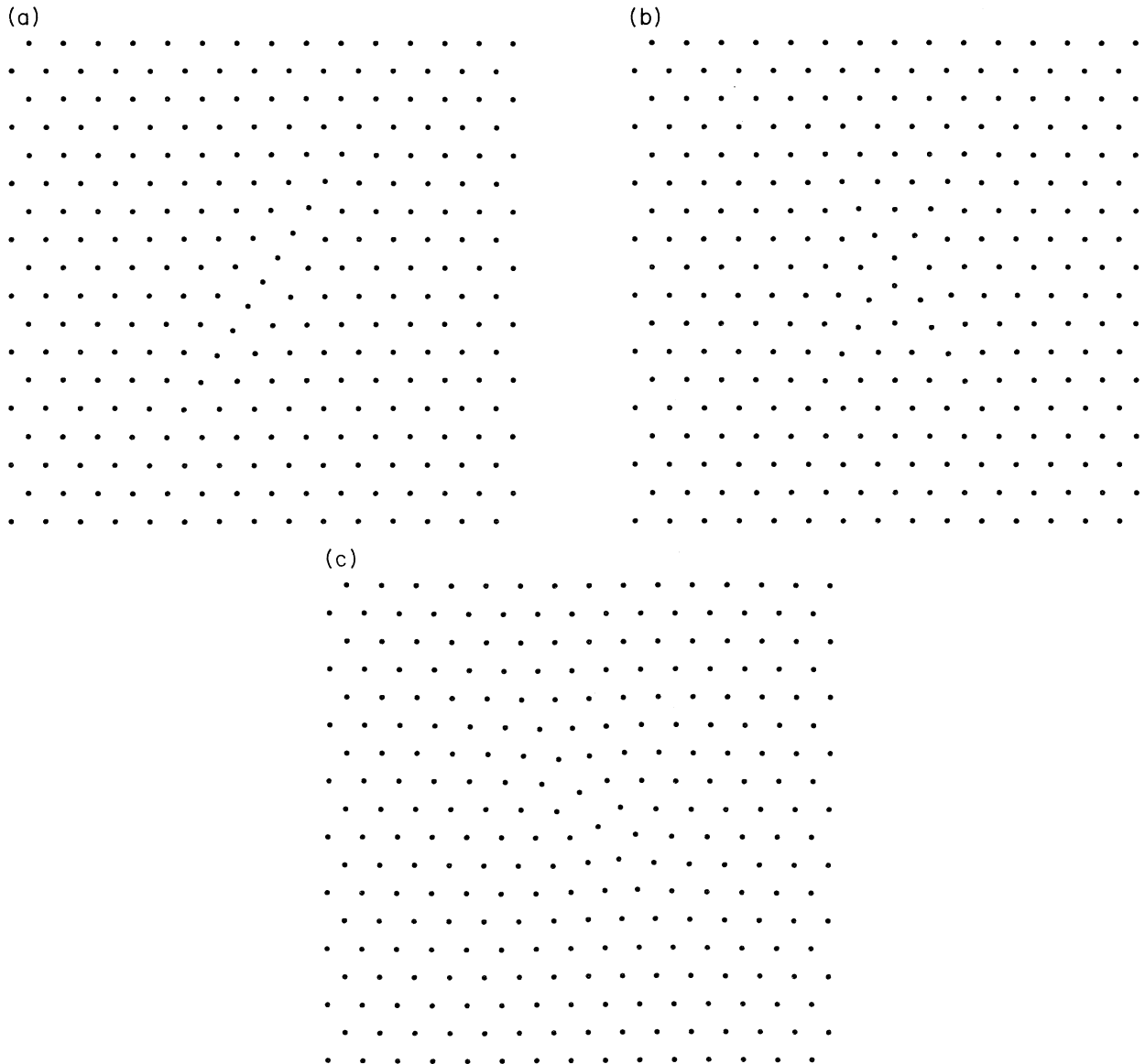


FIG. 4. Relaxed configurations containing (a) EI, (b) CI, and (c) V defects. The point group of the V is C_2 .

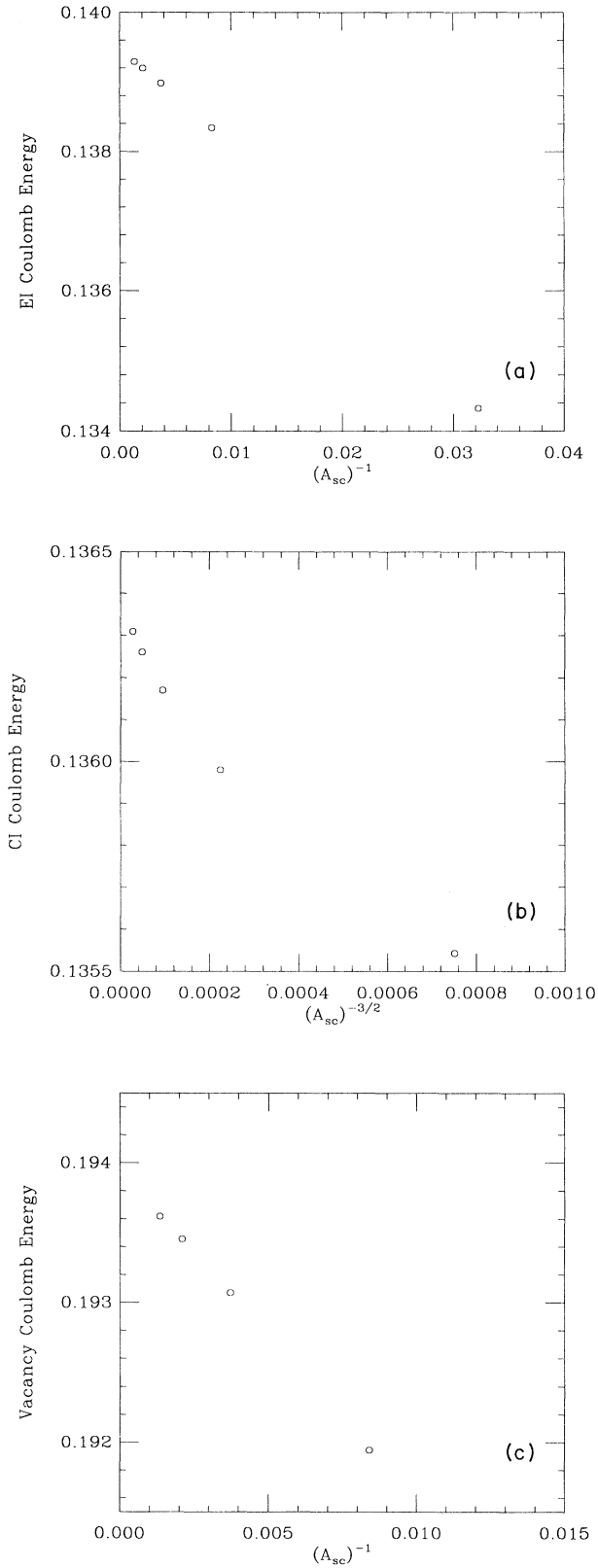


FIG. 5. Defect Coulomb energy vs system size for the (a) EI, (b) CI, and (c) V. The system areas A_{sc} are scaled according to the predictions of elasticity theory.

conclusion of FHM that the EI is stable. We thus omit discussion of the EI in Sec. IV below.

B. Zero-point vibrational energy

Once the equilibrium configuration for each supercell containing a defect is determined, the zero-point vibrational energy is determined by diagonalization of the $2N$ by $2N$ dynamical matrix C . The change in vibrational energy due to the defect is then given by appropriately subtracting the vibrational energy of a perfect lattice:

$$E_{\text{vib}}(\text{defect}) = \frac{\hbar}{2} \left[\sum_{i=1}^{2N} \omega_i(\text{defect}) - \frac{N}{N \pm 1} \sum_{i=1}^{2(N \pm 1)} \omega_i(\text{perfect}) \right]. \quad (14)$$

The comparison is made to a supercell energy, rather than to $2N$ times the perfect lattice zero-point vibrational energy found in Sec. II because the systematic deviations in the vibrational energy calculated over a finite cell as discussed in Sec. II exceed the difference in vibrational energy that we wish to calculate.

The resultant changes in the zero-point vibrational energies for the CI and V systems of $30t^2 \pm 1$ electrons with $t=1,2,3$ are plotted in Fig. 7. We determine a scaling law for the effect of the image defects on the total vibrational energy by assuming that the difference in vibrational energy between the lattice containing periodic defects and the perfect lattice is dominated by vibrational models localized near the defect and representing these modes as fluctuating dipoles located near the defect and its images. The image dipoles provide an effective additional force that scales as $A_{sc}^{-3/2}$, where A_{sc} is the area of the supercell. Thus we expect the effect of the image defects on the frequencies of the local modes to scale as $A_{sc}^{-3/2}$. Extrapolating our results to $A_{sc} = \infty$, we find

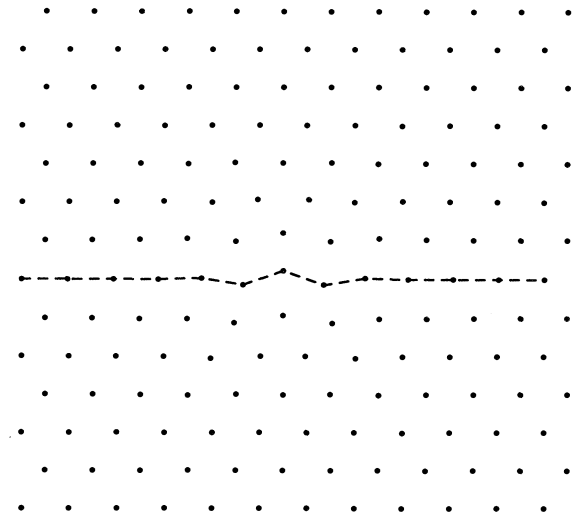


FIG. 6. Unstable “buckling” mode of the EI shown in Fig. 1.

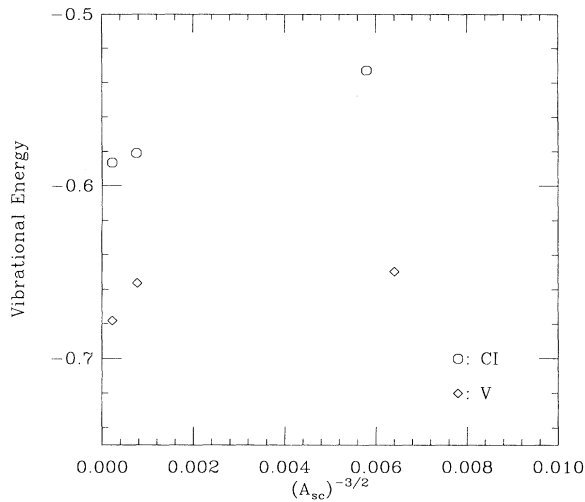


FIG. 7. Change in zero-point vibrational energy with system size for the CI and V defects.

$$C_{3/2}(\text{CI}) = -0.59 \pm 0.01 \text{ and } C_{3/2}(\text{V}) = -0.67 \pm 0.02.$$

Both stable point defects lower the zero-point vibrational energy of the Wigner crystal in the harmonic approximation. For each type of defect, there is a critical density, or

$$r_s(\text{defect}) = \left[\frac{-C_{3/2}(\text{defect})}{C_1(\text{defect})} \right]^2, \quad (15)$$

where the defect energy computed using the first two terms in (11) is zero. Below this density Coulomb forces dominate, an isolated defect raises the energy of the Wigner crystal and the ground state is crystalline. Above this density the zero-point vibrational energy begins to overwhelm the Coulomb energy and a condensation of defects is favored. From our calculations we find $r_s(\text{CI}) = 15 \pm 1$ while $r_s(\text{V}) = 9 \pm 1$, for the critical density. These densities are much higher than the $r_s = 37 \pm 5$ calculated by Tanatar and Ceperley, implying either (1) point defects are not responsible for a continuous melting mechanism and/or (2) the anharmonic terms in the expansion of the defect energies move the critical density nearer the Tanatar and Ceperley value. The energies of the extended defects such as dislocations, disclinations, and grain boundaries that have been investigated in regard to the thermal melting of the Wigner crystal⁴ are not calculated here. Although a dislocation, for example, can be viewed as a semi-infinite line of CI spaced one lattice constant apart, the present work cannot be expected to model the energetics of these defects well, as all point defects studied here are well separated. Anharmonic oscillator terms must be included if our estimate of the crit-

ical r_s is to be improved. Assuming all anharmonic effects are included in the $C_2(\text{defect})$ terms, $C_2 \approx -2.1$ is necessary in order that $r_s(\text{CI})$ equal the Tanatar and Ceperley value of $r_s \approx 37$.

V. POINT DEFECTS: INTERACTION

When elasticity theory is applied to the interaction between a point defect in the 2D Wigner crystal and its images, it predicts an interaction that scales at large separations r as r^{-2} , for a defect of low symmetry, such as the vacancy or EI and as r^{-3} for a defect of higher symmetry, such as the CI.⁴ Our periodic boundary conditions always yield a rectangular superlattice of defects with the two sides of the supercell in the proportional of $3\sqrt{3}$ to 5. As the dimensions of the supercell t are changed only the scale of the superlattice is changed, not its shape. Therefore, regardless of the specific tensor nature of the interaction, the net effect of the supercell size changes should scale exactly the same way with r as the single pair interaction, provided that the minimum separation between defects is in the large separation regime. In Fig. 5, the increase in defect Coulomb energy is plotted against the characteristic interdefect separation length $r = \sqrt{A_{\text{sc}}}$, raised to the power predicted by elasticity theory. The interaction between both EI's and vacancies scale roughly as r^{-2} , as expected, although the three largest systems tested most closely fit an exponent of 2.3 for the vacancy and 2.1 for the EI. The interaction between CI's does not seem to scale as r^{-3} over the range of supercell sizes tested; in fact the form r^{-2} fits better over the system sizes tested. Either the interaction between CI does not scale as r^{-3} at large distances as predicted by elasticity theory, or a separation of 20 to 30 lattice constants is not enough to bring the CI interaction into the large separation regime.

VI. CONCLUSIONS

The energies of point defects in the 2D Wigner crystal have been calculated very accurately. Earlier work on the subject by Fisher, Halperin, and Morf⁴ has been corrected and extended. In particular, we find only one stable interstitial and a lower symmetry for the vacancy. We have also obtained the next term in the large- r_s expansion of the defect energies. This term arises from local zero-point modes and is negative for both of the stable defects.

ACKNOWLEDGMENTS

E. C. was supported in part by the National Science Foundation. V. E. was supported by the Cornell Materials Science Center, the Sloan Foundation, AT&T, the David and Lucile Packard Foundation, and the National Science Foundation Grant No. DMR-8958510.

- ¹E. Wigner, *Phys. Rev.* **46**, 1002 (1934).
- ²C. C. Grimes and G. Adams, *Phys. Rev. Lett.* **42**, 795 (1979).
- ³B. Tanatar and D. M. Ceperley, *Phys. Rev. B* **39**, 5005 (1989).
- ⁴D. S. Fisher, B. I. Halperin, and R. Morf, *Phys. Rev. B* **20**, 4692 (1979).
- ⁵V. Elser, unpublished.
- ⁶D. J. Adams and L R. McDonald, *J. Phys. C* **7**, 2761 (1974).
Further techniques are given for reducing the computation time of Ewald sums.
- ⁷D. Ceperley, *Phys. Rev. B* **18**, 3126 (1978).
- ⁸L. Bonsall and A. A. Maradudin, *Phys. Rev. B* **15**, 1959 (1977).
- ⁹S. L. Cunningham, *Phys. Rev. B* **10**, 4988 (1974).
- ¹⁰W. H. Press, B. P. Flannery, S. A. Teukolsky, and W. T. Vetterling, *Numerical Recipes* (Cambridge University Press, New York, 1986). The subroutine FRPRMN and its associated subroutines were used.